Cite this: DOI: 10.1039/c2nr11947a

www.rsc.org/nanoscale

PAPER

Orthogonally bifunctionalised polyacrylamide nanoparticles: a support for the assembly of multifunctional nanodevices†

F. Giuntini,[a] F. Dumoulin,[b] R. Daly,[c] V. Ahsen,[b] E. M. Scanlan,[c] A. S. P. Lavado,[d] J. W. Aylott,[d] G. A. Rosser,[e] A. Beeby[e] and R. W. Boyle*[a]

Received 8th December 2011, Accepted 18th January 2012
DOI: 10.1039/c2nr11947a

Polyacrylamide nanoparticles bearing two orthogonal reactive functionalities were prepared by reverse microemulsion polymerisation. Water-soluble photosensitisers and peptide or carbohydrate moieties were sequentially attached to the new nanospecies by orthogonal conjugations based on copper-catalysed azide-alkyne cycloaddition and isothiocyanate chemistry.

Introduction

Growing interest in the application of nanotechnology in biomedical research has encouraged great efforts in devising improved materials for the generation of multifunctional nanodevices designed for targeted drug delivery, diagnostic imaging and biosensing. Thanks to favourable physicochemical properties, cross-linked polyacrylamide has gained popularity as a support for biocompatible nanomaterials.[1–9] Polyacrylamide nanoparticles (PANPs) are hydrophilic and give stable colloidal dispersions in water, hence they are suitable for biologic applications. An appealing feature of polyacrylamide nanoparticles is their versatility, resulting from their chemical flexibility. Careful choice of polymerisation conditions, for example, allows control over the size of the resulting nanospecies,[10,11] a parameter that dictates the behaviour of the nanoparticle in living systems, by affecting its cell penetration ability, intracellular localisation, and pharmacokinetic profile (*i.e.*: plasma half-life, distribution and clearance).[12–14] Cargoes can be loaded on polyacrylamide nanoparticles either by encapsulation within the polymer network or by conjugation to reactive functionalities, which can be engineered on the surface of the particle by including suitably functionalised acrylamides in the polymerisation step.[15] Thus, polyacrylamide nanoparticles have been decorated with a wide variety of molecules, including targeting agents (*e.g.*: peptides, carbohydrates, aptamers, oligonucleotides, lipids, *etc.*),[15,16] fluorescent dyes, reporter molecules,[17] drugs, or contrast agents.[18,19]

The field of photodynamic therapy and photodiagnosis greatly benefitted from the advent of nanotechnology.[20–23] The association of photosensitisers with polyacrylamide nanoparticles opened the way to the generation of light responsive nanodevices, which have applications as therapeutic, diagnostic and investigative tools. The incorporation of a photosensitiser into a nanoparticle is an effective way to overcome the poor water solubility displayed by many photosensitisers, to achieve higher loading of photosensitiser in the target cells, and in many instances to prolong the half-life of the photosensitiser in plasma, in particular when the surface of the nanoconjugate is coated with polyethylene glycol (PEG) to delay opsonisation.[24,25]

Luminescent probes and polyacrylamide nanoparticles can also be associated to generate nanosensors for monitoring biological processes in living systems.[26–30] Due to their size, nanosensors allow measurements to be performed within a single cell, with minimal perturbation of the system. In nanosensors, the polymer constituting the core of the particle entraps a fluorescent dye that responds to the variations of the concentration of a given analyte in the intracellular environment by modifying its fluorescence emission profile. Thus, changes in the fluorescence signal following the application of an external stimulus provide real time information on the fluctuations of the level of the analyte, and on the biological processes associated with such fluctuations. The use of nanosensors presents several advantages over the use of stand-alone fluorescent dyes: the choice of the fluorescent probe can be solely based on its sensitivity to the analyte of interest and on its emission profile, because the hydrophilic matrix circumvents all issues related to low water solubility, instability and toxicity of the dye. Once incorporated in the polyacrylamide matrix, even hydrophobic dyes can be used in aqueous solutions, and because interactions of the encapsulated probe with macromolecules are prevented, its degradation by enzymes and its association with proteins or membranes are

[a]*Department of Chemistry, University of Hull, Kingston-upon-Hull, East Yorkshire, HU6 7RX, UK*
[b]*Gebze Institute of Technology, Department of Chemistry, P.O. Box 141, Gebze, 41400, Kocaeli, Turkey*
[c]*School of Chemistry, Centre for Synthesis and Chemical Biology (CSCB), University of Dublin, Trinity College, Dublin, Ireland*
[d]*School of Pharmacy, University of Nottingham, Nottingham, NG7 2RD, UK*
[e]*Department of Chemistry, University of Durham, Durham, DH1 3LE, UK*
† Electronic supplementary information (ESI) available. See DOI: 10.1039/c2nr11947a

reduced. For the same reason, the cell is protected from toxic effect exerted by the dye.

Several examples of nanosensors comprising a nanoparticle and a porphyrinic photosensitiser have been described.[31–39] The majority of such sensors were conceived for the measurement of oxygen concentration inside living cells: platinum complexes of porphyrins, whose phosphorescent lifetime is inversely proportional to the pO_2 in the surrounding microenvironment, are the sensing components of such nanodevices.[32–38]

In the course of our studies concerning the role of reactive oxygen species in cell signalling, we became interested in studying the mobilization of intracellular calcium following singlet oxygen production. We previously reported the synthesis of a nanosensor comprising of a calcium-sensitive fluorophore (calcium green 1, CG-1) embedded in a porphyrin-conjugated polyacrylamide nanoparticle (Fig. 1, A), as a self-standing nanodevice able to elicit a controlled perturbation of the cellular system (production of singlet oxygen) and to register the downstream events of the cellular response to such variation (calcium ion mobilization).[31]

With the aim of improving cellular delivery of the nanosensors, we reasoned that a cell penetration enhancing moiety or a targeting agent could be conjugated to the surface of the nanodevice alongside the porphyrin, provided a second reactive functionality could be introduced on the polymer. (Fig. 1, B). In order to maintain control over the selectivity of the conjugations, the two reactive functionalities displayed on the new nanoparticles would need to display no overlapping reactivity, so that either one of them could be selectively conjugated to a given cargo.

The functionalisation of polyacrylamide nanoparticles with amino groups is widely documented.[8,17,18,31,40,41] To generate these species, a suitable acrylamide containing an amino-group is copolymerised with acrylamide and *N*,*N*-methylenebisacrylamide as the cross-linker, under reverse-phase microemulsion polymerisation conditions. The relative amount of cross-linker used during the polymerisation can be varied to fine tune the structure of the nanogel and the properties of the nanospecies generated (pore size, elasticity, swelling, *etc.*).[40–42]

Numerous examples of efficient decoration of amino-functionalised polyacrylamide nanoparticles with cargoes of diverse nature are reported in the literature.[8,17,18,31,43,44]

We have previously shown that porphyrins bearing an isothiocyanate group or a hydroxysuccinimide-activated carboxylic function can be attached to the surface of amino-functionalised polyacrylamide nanoparticles.[4,31] The synthesis of nanoparticles bearing alkyne or azide groups, reactive under CuAAC conditions, was also reported:[45–47] in particular, we have shown that alkyne-functionalised polyacrylamide nanoparticles successfully undergo conjugation with TAMRA derivative and peptidocoumarins in the presence of tetrakis(acetonitrile) copper(I) hexafluorophosphate and TBTA.[48] In these reports, the introduction of the functional groups on the particle surface was achieved *via* a common strategy, *i.e.* by adding the functionalised acrylamide to the polymerisation mixture. On the basis of these studies, we envisaged that the combined use of amino- and azido- (or alkyne)-bearing acrylamides during the polymerisation step would afford nanospecies displaying the two required orthogonal functionalities which, under the appropriate conditions, could selectively take part in conjugation with different cargoes.

Several examples of polymers prepared under controlled polymerisation conditions (living free-radical polymerisation) and displaying orthogonal functionalities have been reported in the literature,[49–55] but to the best of our knowledge it has never been exploited for the assembly of multifunctional polyacrylamide nanospecies under reverse phase microemulsion polymerisation.

Results and discussion

While *N*-(3-aminopropyl)methacrylamide hydrochloride is a commercially available compound, no acrylamide functionalised with an azide or a triple bond can be purchased. Therefore we first focused on the synthesis of two acrylamide monomers with comparable chain lengths, bearing the desired groups. Amino-azide **1** in its Boc-protected form was obtained starting from 2-(2-aminoethoxy)ethanol in two steps on a multi-gram scale.[56] Boc-protected amino-alkyne **2** was also obtained in two steps from ethanolamine. The desired acrylamides **3** and **4** were prepared in moderate yields by reaction of **1** and **2** with acryloyl chloride following HCl-mediated Boc-deprotection. (Scheme 1).

Acrylamides **3** and **4** were efficiently incorporated into polyacrylamide nanoparticles under reverse-phase microemulsion polymerisation conditions.[27,48] (Scheme 2, Box 1) The desired nanospecies **5** and **6** were obtained in 81 and 88% yield, respectively. IR spectra of the particles obtained showed a band at 2111

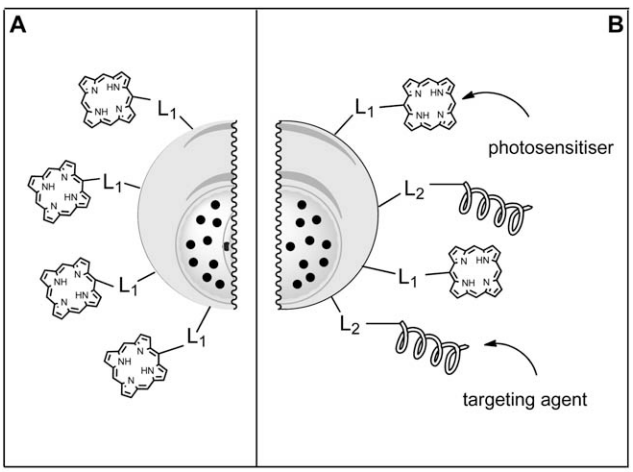

Fig. 1

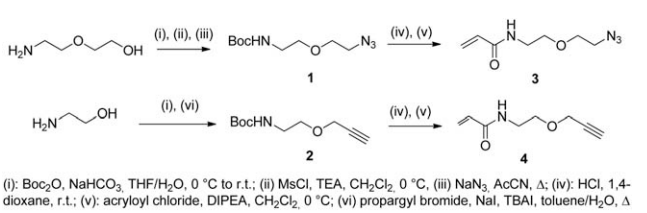

Scheme 1

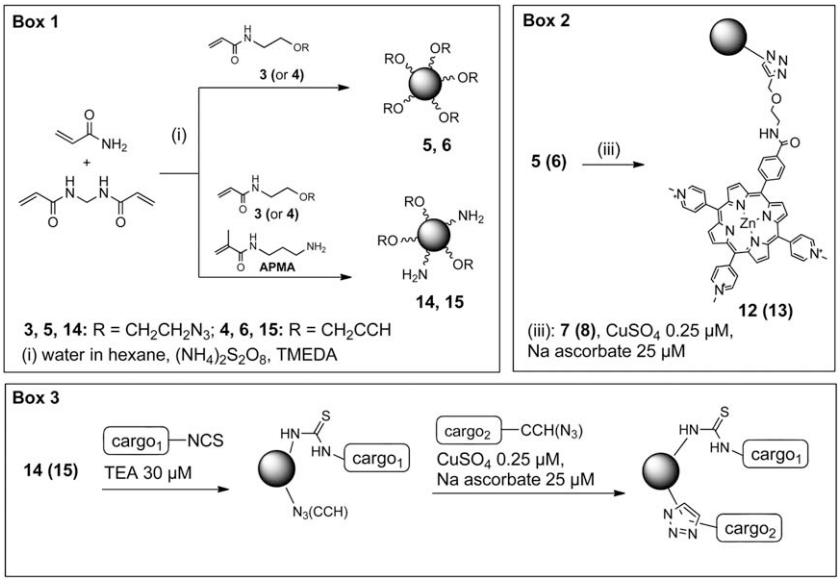

Scheme 2

cm^{-1} for **5**, which is diagnostic for the stretching of N–N bond in the azido groups, and a very weak band at 2090 cm^{-1} for **6**, generated by the stretching of the triple bonds.

A further confirmation of the presence of the desired reactive functionalities on the nanoparticles was provided by the successful conjugation of **5** and **6** with "clickable" porphyrins **7** and **8**, respectively, under Cu(I)-catalysed triazole formation conditions.[57] Alkyne-bearing porphyrin **7** and azide-bearing porphyrin **8** were obtained by coupling hydroxysuccinimido-ester **9** with amines **10** and **11** in $NaHCO_3$ buffer. (Scheme 3) The choice of using **7** and **8** as zinc complexes was made in order to prevent the sequestration of copper ions by the macrocycle during CuAAC. The conjugation reaction occurred smoothly in water at room temperature, in the presence of $CuSO_4$ and sodium ascorbate. (Scheme 2, Box 2) Gel filtration on Sephadex G25 provided an expeditious mean to separate the nanoconjugates from the catalysts and non-reacted porphyrin.[58] Nanoconjugates **12** and **13** were recovered in 95 and 83% yields, respectively, following precipitation with ethanol and filtration.

Having verified the usefulness of acrylamides **3** and **4** for the introduction of azides and terminal alkynes on polyacrylamide nanoparticles, we turned our attention to the preparation of doubly-functionalised species. To this end, we modified the protocol by replacing the 1% of functionalised acrylamide in the mixture of monomers with 0.5% of *N*-(3-aminopropyl)meth-acrylamide hydrochloride (**APMA**) and 0.5% of either **3** or **4**. We were pleased to observe that in both cases the polymerisation afforded bifunctionalised nanospecies **14** and **15** (Scheme 2), whose average hydrodynamic diameter did not differ signifi-cantly from the diameter exhibited by the monofunctionalised

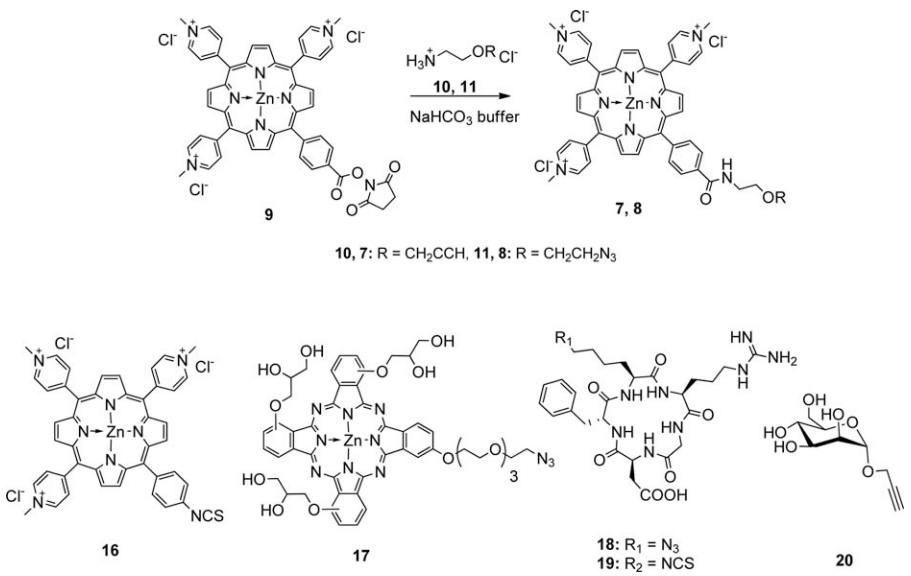

Scheme 3

particles. (Table 1). The presence of the alkyne and azide functionalities was again verified by IR, while the presence of the amino group was revealed by means of fluorescamine staining.[59]

With the aim of assessing the versatility of the new bifunctionalised polyacrylamide nanospecies, and to verify the feasibility of orthogonal sequential double-conjugations, we selected a group of conjugatable molecules to decorate the particles. (Scheme 4) Bearing in mind that this work originated from the need of associating nanoparticles with both photosensitisers and cell-penetration or cell-targeting entities, we selected a small group of molecules representative of both groups. Porphyrins **7**, **8**, and **16**,[60] and phthalocyanine **17** were chosen as examples of photosensitisers, whereas RGD-containing cyclo-pentapeptides **18** and **19** and 1-propargyloxymannose **20** as models for targeting moieties. Although RGD-containing peptides[8,46,61–65] and mannose[66–69] have already been used in association with a variety of nanoparticles to improve their receptor-mediated targeting and cellular uptake, in this work they were selected as models to study the feasibility of the conjugation of peptides and carbohydrates to the new doubly-functionalised nanospecies. As shown in Scheme 3, all the molecules selected were engineered to display groups which would provide them with reactivity towards amines, azides, or triple bonds. With "clickable" porphyrins **7** and **8** already in our hands, we chose isothiocyanato porphyrin **16** as an amino-reactive photosensitiser. Porphyrin **16** was prepared in quantitative yield by metallation of the corresponding free base in 10 mM $NaHCO_3$ buffer. Although the conjugation of **16** to amino-functionalised nanoparticles does not require the presence of metal ions in the reaction mixture, the use of a zinc-porphyrin was necessary because the resulting nanoconjugate would be exposed to copper ions under the CuAAC conditions of the second ligation step. RGD-containing cyclopentapeptides were synthesised by Fmoc-SPPS, according to literature procedures.[70] The azide group was incorporated in peptide **18** by coupling Fmoc-ε-azidolysine[71] during chain elongation, whereas the isothiocyanate function of **19** was installed on the side chain of Lys by treatment of the corresponding amino-derivative with 1,1′-thiocarbonyldi-2(1*H*)pyridone.[72]

Because amino-functionalised polyacrylamide nanoparticles have been reported to be prone to irreversible aggregation,[48] a behaviour that has been ascribed to the Michael addition of the amino-groups onto residual acrylamide moieties on the surface of the particle, we envisaged that the attachment of the amino-reactive cargo should be carried out before the CuAAC conjugation. (Scheme 2, Box 3).

Thus, nanoparticles **15** were first treated with isothiocyanate porphyrin **16** in the presence of 30 μM triethylamine. The resulting porphyrin-conjugated particles **21** were then exposed to azide-functionalised cyclopentapeptide **18** under the conditions described above. The doubly-decorated nanospecies **22** were obtained in 75% yield over two steps. Exchanging the reactive functionalities on the cargo molecules did not hamper the double conjugation, as we confirmed by exposing particles **15** first to cyclopentapeptide isothiocyanate **19** to afford conjugate **23**, and then to porphyrin **8** to give nanospecies **24**. The final nanoconjugate was obtained in 63% overall yield. (Scheme 4) A similar conjugate was obtained starting from particles **14**, which reacted with cyclopentapeptide **19** in the presence of triethylamine, yielding **25**, and subsequently with porphyrin **7** under CuAAC conditions to give conjugate **26**, confirming that the reactivity of the azide group is maintained on the bifunctionalised nanoparticles. (Fig. 2) Treatment of nanospecies **27**, obtained by reaction of porphyrin **16** on particles **14**, with 1-propargyloxymannose **20**[12] under CuAAC conditions yielded conjugate **28** in 90% yield. Treatment of nanoconjugate **23** with azido-phthalocyanine **17**[73] in 10% aqueous DMSO in CuAAC conditions, gave nanoparticles **29** in 91% yield. Fig. 2 summarises the nanoconjugates obtained by applying the protocols devised with bifunctionalised nanoparticles and different permutations of the conjugatable molecules we selected.

Table 1

Particles	Yield (%)	Z_{ave} (nm)
5	81	37.6
6	88	40.0
14	92	43.8
15	87	39.8
30	92	37.7

Characterisation of the nanoconjugates

The hydrodynamic size of the nanoconjugates was measured by photon correlation spectroscopy. (Table 1 and Table 2). The conjugated nanospecies showed a marked increase in hydrodynamic radius compared to the native particles. These observations are in agreement with our previous findings,[4] and can be explained on the basis of the increased thickness of the counterions corona tightly associated with the nanoparticle, caused by the covalent ligation of tri-cationic molecules on the surface of the gel.[74,75] The presence of positive charges could also cause the swelling of particles because of the increased osmotic pressure in the proximity of the nanogel.[76] The efficiency of the attachment of the photosensitisers to the particles was evaluated by UV-visible spectroscopy. The UV-visible spectra of particles **22** and particles **29** show the typical profiles of metal complexes of porphyrins and phthalocyanines. (Fig. 3) To reveal the presence of mannose on particles **28** we relied on a colorimetric test based on the reaction of carbohydrates with phenol in the presence of concentrated sulfuric acid, described by Masuko *et al.*[77] The presence of mannose is evidenced by the development of a broad band centred at 470–480 nm in the absorption spectrum. (Fig. 4) A similar assay has been previously used to estimate the loading of mannose on mesoporous silica nanoparticles.[68] The presence of peptides **18** and **19** on nanoparticles was detected with the Sakaguchi test,[78] which reveals the presence of guanidine on the side-chain of Arg. (Fig. 5) An application of this assay to detect the presence of RGD-containing peptides anchored on a solid support has been reported previously.[79] The tests described above were intended to be qualitative assays, aimed at verifying the effectiveness of the conjugation reactions. The results obtained confirmed that the presence of the first cargo on the particle does not prevent the attachment of the second one, indicating that the reactivity of the two groups is maintained throughout the whole conjugation process.

Following our original concept of obtaining doubly-conjugated Ca-sensing nanoparticles, we prepared nanoparticles **30**, displaying alkyne and amine groups and entrapping

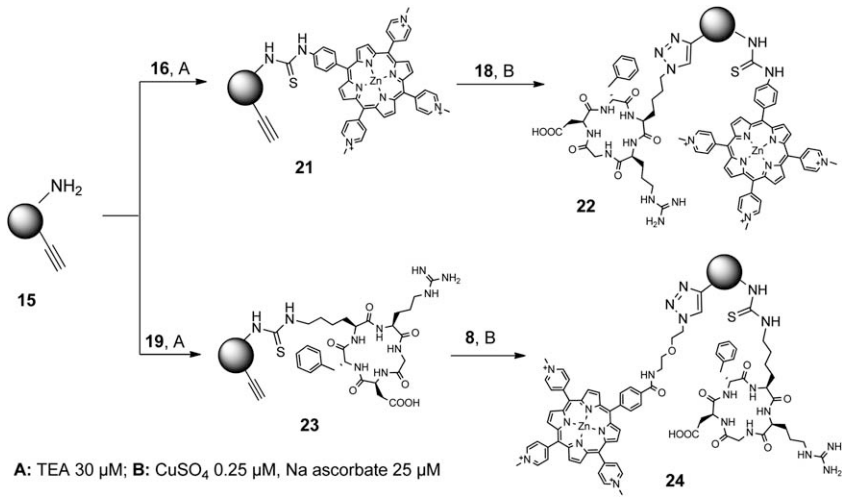

Scheme 4

dextran-supported CG-1.[31] (Scheme 5) The two conjugation steps required for the preparation of nanoconjugates **31** were performed sequentially, without isolating the intermediate conjugate. (Scheme 5) To this end, particles **30** were first treated with porphyrin **16** in the presence of triethylamine, and then peptide **18**, $CuSO_4$ and sodium ascorbate were added to the aqueous solution of the conjugated nanospecies, after gel filtration. The presence of both cargoes was verified as described above. The sensors show a linear response to the increasing calcium concentration over the range of 0–12 nM ($y = 0.942x + 134.85$, $R^2 = 0.9799$). These results are in agreement with data previously generated, confirming that embedding CG-1 within porphyrin-coated polyacrylamide nanoparticles does not impair its sensitivity to calcium ions in the surrounding environment.[31]

Table 2

Particles	Yield (%)	Z_{ave} (nm)	Particles	Yield (%)	Z_{ave} (nm)
12	95	102.3	**25**	74	103.1
13	83	92.3	**26**	97	92.7
21	82	99.8	**27**	79	110.1
22	92	96.9	**28**	90	98.4
23	70	89.5	**29**	91	69.2
24	90	70.0	**31**	88	71.7

Conclusions

This work shows that the insertion of two orthogonal functionalities on polyacrylamide nanoparticles can be achieved, and that the reactivity of such groups can be successfully exploited to sequentially load the particles with two different cargoes. To the best of our knowledge this represents the first example of the application of orthogonal conjugation on polyacrylamide nanoparticles. The insertion of the two reactive groups on the particle is achieved *via* standard reverse phase microemulsion polymerisation techniques, yet it gives access to nanodevices with a high degree of functionalisation and complexity. The mild reaction protocols and expeditious purification make this novel approach especially suitable for the conjugation of biomolecules

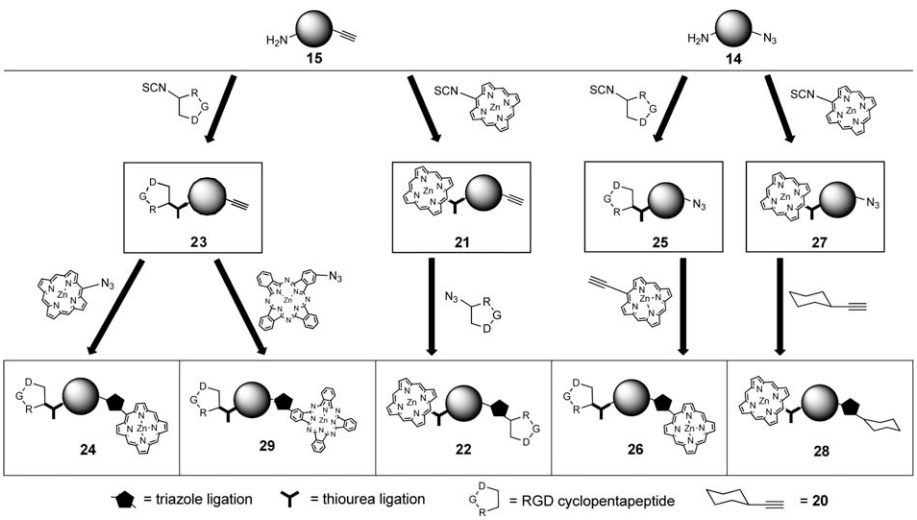

Fig. 2

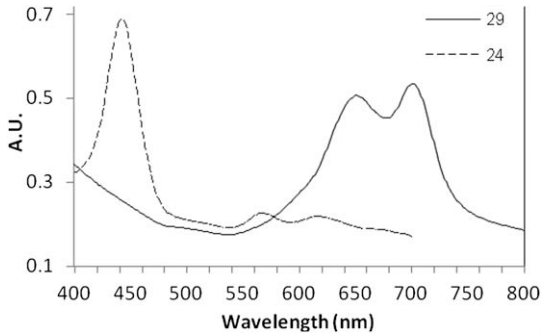

Fig. 3

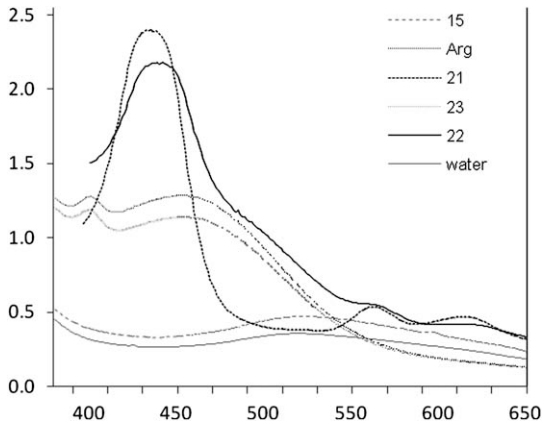

Fig. 4 Absorption spectra obtained after Sakaguchi test.

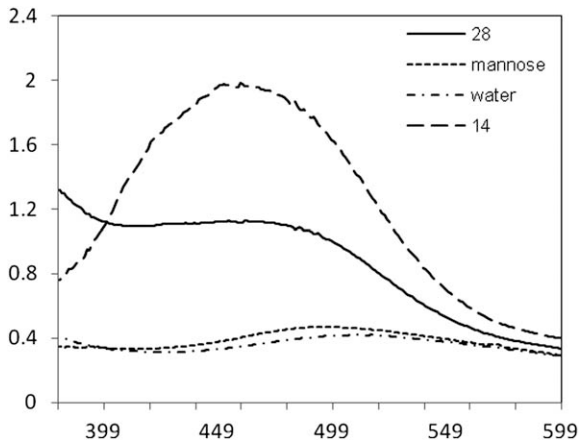

Fig. 5 Absorption spectra obtained after Masuko test.

to nanoparticles; however we anticipate that this method will have a broad relevance, because it will be applicable to conjugate cargoes of different nature to a wide variety of polymeric nanoparticles.

Experimental

General remarks

^{1}H and ^{13}C NMR spectra were recorded on JEOL Eclipse 400 and JEOL Lambda 400 spectrometers (operating at 400 MHz for ^{1}H and 100 MHz for ^{13}C). $CDCl_3$, DMSO-d_6, and MeOH-d_3 were used as solvents. Chemical shifts (δ) are reported in parts per million (ppm), referenced to either $CHCl_3$ (^{1}H, 7.26 ppm; ^{13}C, 77.16 ppm) or DMSO (^{1}H, 2.50 ppm; ^{13}C, 39.52 ppm) or MeOH (^{1}H, 3.31 ppm; ^{13}C, 49.00 ppm). Coupling constants (J) are recorded in Hz and significant multiplicities described by singlet (s), doublet (d), triplet (t), quadruplet (q), broad (br), multiplet (m), or doublet of doublets (dd). A Malvern Photon Correlation Spectrometer equipped with a 70 mW blue laser operating at 470 nm at an angle of 90° was used for the PCS measurements. The measurements were performed at room temperature, at a concentration of 5 mg mL^{-1} of nanospecies in 7 mM aqueous NaCl, unless otherwise stated, and the solutions were filtered through a 0.22 μm filter (Millex GP) previous to the measurements. CI, EI, and pAPCI mass spectra were performed at the EPSRC Mass Spectrometry Service (Swansea). ESI mass spectra were performed on a Varian 500-MS ion trap spectrometer, equipped with a Varian Prostar 212LC binary gradient pumping system and a Varian ProStar 410 autosampler. A standard Varian ESI source was used operating in +ve ion mode. Data was acquired and processed using Varian Workstation software. MALDI mass spectra were performed on a Bruker Reflex IV MALDI-TOF, operated in reflectron mode and monitoring positive ions. Data is acquired and processed using Bruker Compass software. 1,8-Dihydroxy-9,10-dihydroanthracen-9-one (dithranol) was used as the matrix. UV–visible spectra were recorded on a Varian Cary spectrophotometer. Fluorescence spectra were recorded on a Cary Eclipse Fluorimeter. Flash chromatography was carried out on silica gel 60 (MP Biomedicals, 32 −63 μm). Analytical TLC was carried out on aluminium sheets pre-coated with silica gel 60 (Fluka, 0.2 mm thick). Commercial solvents and reagents were used without further purification unless stated otherwise. Porphyrins 5-(4-isothiocyanatophenyl)-10,15,20-*tris*-[(4-methylpyridynium)yl]porphyrin trichloride and 5-[4-(succinimide-*N*-oxycarbonyl)phenyl]-10,15,20-*tris*-[(4-methylpyridynium)yl] porphyrin trichloride were prepared according to literature procedures.[60]

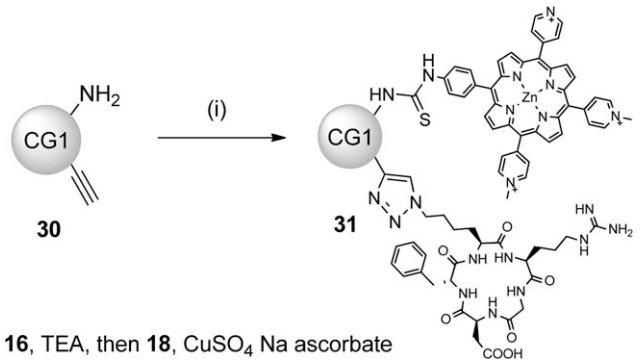

Scheme 5

Chemical reagents were purchased from Sigma-Aldrich, Fluka, Acros, Lancaster, Alfa Aesar, TCI Europe, and Novabiochem at the highest grade of purity available, and were used as received, unless otherwise stated. Dichloromethane and THF were dried by filtration through alumina and storage over

activated molecular sieves.[80] All other solvents were purchased from Fisher Scientific and used as received. Deionised water was obtained from a Millipore Milli-Q system. Gel filtrations were performed on Sephadex® G-25 medium, using pre-packed PD-10 columns (GE Healthcare, UK), using deionised water as the eluent. Filtrations through membranes were performed on Sartolon® polyamide filters, 25 mm, 0.20 μm pores. Solid phase extractions were performed on Supelco Discovery DSC-18 cartridges (1 g). RP-HPLC analyses were performed on a system consisting of a Perkin Elmer series 200 LC pump, and a Perkin Elmer 785A UV/vis detector. The separations were performed on a Gemini C18, 5 μ, 150 × 4.6 mm, 110 Å (Phenomenex, UK), equipped with a SecurityGuard C18 (ODS) 4 × 3.0 mm ID guard column (Phenomenex, UK) at a flow rate of 1 mL min^{-1}. The mobile phase consisted of 0.1% TFA in water (solvent A) and 0.1% TFA in acetonitrile (solvent B). Gradient: 0.0–10.0 min 0–95% solvent B, 10.0–15.0 min 95% solvent B, 15.0–15.1 min at 95–5% solvent B, 15.1–18.0 min 5% solvent B.

General procedure for the synthesis of functionalised acrylamides: 2-(2-azidoethoxy)ethyl acrylamide 3

2-(2-azidoethoxy)-*N*-*t*-butoxycarbonylethylamine (460 mg, 2 mmol) was treated with 4 M HCl in 1,4-dioxane (1 mL, 4 mmol). The resulting solution was stirred at room temperature for 1 h, and the solvent was evaporated. The residue was triturated with diethyl ether and thoroughly dried *in vacuo*. The solid residue was taken in dry DCM and the resulting solution was maintained in an Ar atmosphere and cooled at 0 °C. Triethylamine (613 μL, 4.4 mmol) was added to the solution, followed by dropwise addition of acryloyl chloride (194 μL, 2.4 mmol). The mixture was stirred for 4 h, while being allowed to reach room temperature, then it was diluted with DCM, and washed with 0.1 M aqueous HCl, and with brine. The organic layer was dried ($MgSO_4$) and the solvent was evaporated. The desired compound was isolated by column chromatography (DCM/Et_2O = 1/1), yielding a pale yellow liquid (168 mg, 50%). ^{1}H NMR: ($CDCl_3$) δ: 6.30 (1H, dd, J_{trans} 16.9, J_{gem} 2.7, C*H*HCHCONHR), 6.11 (1H, dd, J_{trans} 16.9, J_{cis} 10.3, $CH_2CHCONHR$), 6.00 (1H, bs, NH), 5.65 (1H, dd, J_{cis} 10.3, J_{gem} 2.7, CH*H*CHCONHR), 3.69 (2H, t, *J* 4.4, CONHCH_2CH_2OR), 3.62–3.55 (4H, m, CONHCH_2CH_2OCH_2R), 3.38 (2H, t, J 3.8, ROCH_2C$H_2$$N_3$); ^{13}C NMR: ($CDCl_3$) δ: 165.5, 130.7, 126.5, 70.2, 67.8, 50.6, 39.1 pAPCI-MS (*m*/*z*): calcd. for $C_7H_{13}N_4O_2$: 185.1033; found: 185.1029 $[M + H]^+$.

2-(prop-2-ynyloxy)ethyl acrylamide 4

Scale: 2 mmol, yield 34%, 52.3 mg, pale yellow fluid.

^{1}H NMR: ($CDCl_3$) δ: 6.29 (1H, dd, J_{trans} 12.9, J_{gem} 1.2, C*H*HCHCONHR), 6.11 (1H, dd, J_{trans} 12.9, J_{cis} 7.7, $CH_2CHCONHR$), 6.0 (1H, bs, NH), 5.65 (1H, dd, J_{cis} 7.7, J_{gem} 1.2, CH*H*CHCONHR), 4.19 (2H, s, ROCH_2CCH), 3.65 (2H, t, *J* 3.5, NHCH_2CH_2O), 3.58 (2H, t, *J* 3.5, NHCH_2CH_2O), 2.47 (1H, s, CC*H*); ^{13}C NMR: ($CDCl_3$) δ: 165.5, 130.7, 126.5, 79.3, 74.8, 68.6, 58.3, 39.1 CI-MS (*m*/*z*): calcd. for $C_7H_{12}NO_2$: 154.0863; found: 154.0863 $[M + H]^+$.

General procedure for the synthesis of functionalised water soluble porphyrins from derivative 9: 5-{4-[2-(prop-2-ynyloxy) ethyl]phenyl}-10,15,20-*tris*-[(4-methylpyridynium)yl]porphyrin trichloride 7

2-(prop-2-ynyloxy)-*N*-*t*-butoxycarbonylethylamine (40 mg, 0.2 mmol) was treated with 4 M HCl in 1,4-dioxane (0.5 mL, 2.0 mmol). The resulting solution was stirred at room temperature for 1 h, and the solvent was evaporated. The residue was triturated with diethyl ether and thoroughly dried *in vacuo*. To the residue, porphyrin NHS (77 mg, 0.08 mmol) was added, followed by 0.1% (w/v) aqueous $NaHCO_3$ (5 mL). The resulting mixture was stirred for 1 h, at room temperature, poured in 10% aqueous NH_4PF_6 (25 mL), and the precipitate formed was collected by filtration through paper. The solid was dissolved in acetone (30 mL) and the precipitation of desired compound was promoted by addition of a 20% solution of TBAC in acetone (3 mL). The solid was collected by filtration and was crystallised from methanol/diethyl ether. (Dark purple solid, 37 mg, 49%). HPLC: t_R: 6.00 min.

^{1}H NMR: (*DMSO-d*$_6$) δ: 9.57–9.57 (6H, *10 + 15 + 20-m-Ar*), 9.17 (6H, br, *β-H*), 9.07–9.00 (m, 8H, *β-H* and *10 + 15 + 20-o-Ar*), 8.40 (2H, d, *J* 7.7, *5-o-Ar*), 8.32 (2H, d, *J* 7.7, *5-m-Ar*), 4.78–4.76 (9H, m, s, *CH*$_3$), 4.27 (2H, br, OCH_2CCH), 3.75–3.72 (2H, m, NHCH_2CH_2O), 3.63–3.62 (2H, m, NHCH_2CH_2O), 3.55–3.54 (1H, m, OCH_2CC*H*); ^{13}C NMR: (*DMSO-d*$_6$) δ: 166.0, 156.4, 144.2, 143.0, 134.1, 132.0, 126.1, 121.8, 115.4, 114.8, 80.4, 77.3, 67.8, 57.4, 47.8; MALDI-MS (*m*/*z*): calcd. for $C_{50}H_{45}N_8O_2$: 789.3649, found: 789.3634 $[M\text{-}3Cl + 2H]^+$. UV/vis: (H_2O) λ (%): 421 (100), 518 (6.4), 556 (2.8), 583 (3.5), 639 (1.9); log ε_{421}: 5.31.

5-{4-[2-(2-azidoethoxy)ethyl]phenyl}-10,15,20-*tris*-[(4-methylpyridynium)yl]porphyrin trichloride 8

Scale: 0.1 mmol, 52 mg, 56%, dark purple solid. ^{1}H NMR: (*DMSO-d*$_6$) δ: 9.55–9.52 (6H, *10 + 15 + 20-m-Ar*), 9.16 (br, 4H, *β-H*), 9.07–9.00 (m, 10H, *β-H* and *10 + 15 + 20-o-Ar*), 8.38 (2H, d, *J* 9.2), 8.32 (2H, d, *J* 9.2), 4.75–4.74 (9H, m, s, *CH*$_3$), 3.75–3.73 (4H, m, CONHCH_2CH_2OCH_2R), 3.65–3.62 (2H, m, CONHCH_2CH_2OCH_2R), 3.49 (2H, t, *J* 4.7, ROCH_2C$H_2$$N_3$), -3.02 (2H, s, *pyrrole NH*); ^{13}C NMR: (*DMSO-d*$_6$) δ: 166.1, 156.5, 156.4, 144.2, 143.0, 134.2, 134.1, 132.1, 126.1, 121.9, 115.4, 114.7, 69.0, 68.8, 50.1, 47.8; MALDI-MS (*m*/*z*): calcd. for $C_{49}H_{45}N_{11}O_2$: 819.3741, found: 819.4056 $[M\text{-}3Cl + H]^+$; UV/vis: (H_2O) λ (%): 423 (100), 519 (6.4), 560 (3.0), 585 (3.5), 640 (2.0); log ε_{423}: 5.34.

General procedure for the complexation of cationic porphyrins: 5-(4-isothiocyanatophenyl)-10,15,20-*tris*-[(4-methylpyridynium) yl]porphyrinato zinc(II) trichloride

An aqueous solution (10 mL) of **16** (63 mg, 0.07 mmol), was treated with $ZnOAc_2$ (20 mg, 0.1 mmol), and the resulting mixture was stirred at room temperature for 10 min. A 10% (w/v) aqueous solution of NH_4PF_6 (10 mL) was added to the reaction mixture and the resulting suspension was centrifugated. The precipitate was dissolved in acetone (10 mL) and the precipitation of the desired porphyrin was promoted by addition of a 20% solution of TBAC in acetone (1 mL). The solid was recovered by filtration and crystallised from methanol/diethyl ether. (Green solid, 56 mg, 90%). HPLC: t_R: 6.50 min; ^{1}H NMR: (*DMSO-d*$_6$) δ:

9.33–9.31 (6H, *10 + 15 + 20-m-Ar*), 9.13–9.11 (4H, m, *β-H*), 9.03–8.99 (4H, *β-H*), 8.91–8.89 (6H, *10 + 15 + 20-o-Ar*), 8.54 (2H, d, *J* 8.3, *5-o-Ar*), 8.40 (2H, d, *J* 8.3, *5-m-Ar*), 4.8 (9H, s, CH_3); ^{13}C NMR: (*DMSO-d*$_6$) *δ*: 172.2, 161.3, 151.8, 150.3, 150.2, 149.9, 144.8, 136.2, 134.7, 134.1, 133.6, 133.3, 132.8, 129.7, 116.8; MALDI-MS (*m/z*): calcd. for $C_{45}H_{33}N_8SZn$: 781.1824, found: 781.2476 [M- 3Cl + H]$^+$; UV/vis: (H_2O) λ (%): 435 (100), 565 (8.6), 607 (5.5); log ε_{435}: 5.09.

5-{4-[2-(2-azidoethoxy)ethyl]phenyl}-10,15,20-*tris*-[(4-methylpyridynium)yl]porphyrinato zinc(II) trichloride

Green solid. Scale: 0.65 mmol, yield 91%, 58 mg. HPLC: t_R: 6.15 min; ^{1}H NMR: (MeOH-*d*$_3$) *δ*: 9.35–9.31 (6H, m, *10 + 15 + 20-m-Ar*), 9.12 (4H, s, *β-H*), 9.01–8.97 (4H, s, *β-H*), 8.92–8.88 (6H, m, *10 + 15 + 20-o-Ar*), 8.27–8.21 (4H, m, *5-o-Ar* and *5-m-Ar*), 4.79 (9H, s, CH_3), 3.78–3.72 (6H, m, $CONHCH_2CH_2OCH_2CH_2N_3$), 3.42 (2H, t, *J* 4.9, $ROCH_2CH_2N_3$); ^{13}C NMR: (MeOH-*d*$_3$) *δ*: 167.3, 158.5, 149.3, 147.4, 147.3, 146.9, 143.9, 142.0, 141.9, 132.7, 131.8, 131.2, 130.6, 130.4, 129.6, 123.9, 121.5, 113.9, 113.1, 68.1, 67.6, 49.1, 38.2; MALDI-MS (*m/z*): calcd. for $C_{49}H_{42}N_{11}O_2Zn$: 880.2800, found: 880.3026 [M- 3Cl]$^+$. UV/vis: (H_2O) λ (%): 434 (100), 564 (7.2), 606 (3.2); log ε_{434}: 5.26.

5-{4-[2-(2-propynyloxy)ethyl]phenyl}-10,15,20-*tris*-[(4-methylpyridynium)yl]porphyrinato zinc(II) trichloride

Green solid. Scale: 0.45 mmol, yield 93%, 39 mg. HPLC: t_R: 5.98 min; ^{1}H NMR: (MeOH-*d*$_3$) *δ*: 9.35–9.32 (6H, m, *10 + 15 + 20-o-Ar*), 9.31–9.10 (4H, s, *β-H*), 8.98 (4H, s, *β-H*), 8.91–8.89 (6H, m, *10 + 15 + 20-m-Ar*), 8.30–8.23 (4H, m, *5-o-Ar* and *5-m-Ar*), 4.29 (2H, d, *J* 2.9, OCH_2CCH), 3.84 (2H, t, *J* 5.5, $NHCH_2CH_2O$), 3.75 (2H, t, *J* 5.5, $NHCH_2CH_2O$), 2.92 (1H, t, *J* 2.9, OCH_2CCH); ^{13}C NMR: (MeOH-*d*$_3$) *δ*: 169.7, 160.7, 151.6, 151.5, 149.6, 149.5, 149.2, 146.3, 144.2, 134.7, 133.4, 133.4, 132.8, 132.6, 131.9, 128.1, 126.1, 116.1, 115.3, 80.0, 75.4, 68.7, 58.3, 57.7, 40.3; MALDI-MS (*m/z*): calcd. for $C_{50}H_{41}N_8O_2Zn$: 849.2627, found: 849.2728 [M-3Cl]$^+$; UV/vis: (H_2O) λ (%): 434 (100), 564 (9.8), 608 (6.6); log ε_{434}: 5.27.

General procedure for solid-phase peptide synthesis. H-D(tBu)fK(ε-N$_3$)R(Pmc)G-OH

The synthesis of the protected cyclopentapeptides was accomplished according to the Fmoc/*t*-Bu strategy manually in a 6 mL fritted SPE tube (Supelco, UK), equipped with a cap and plastic valve (Chromabond, UK). Loading of the resin was achieved by treating 2-chlorotrityl chloride polystyrene resin (1 g, 1.4 mmol) with a solution of N-α-Fmoc-glycine (832 mg, 2.8 mmol) and DIPEA (1950 μL, 11.2 mmol) in dry DCM (10 mL) for 60 min. Unreacted sites on the resin were capped by treatment with a solution of DCM/MeOH/DIPEA (3 : 1 : 0.5 v/v/v, 2 × 15 min). The first residue loading was measured spectrophotometrically, and was estimated to be 1.37 mmol g^{-1}. Coupling reactions were performed by treating the resin (400 mg) with a solution of Fmoc-amino acid (2 equiv relative to the resin loading), PyBOP (1.9 equiv) and diisopropylethylamine (4 equiv) in DMF (10 mL g^{-1} resin) for 60 min. The efficiency of the coupling reactions was assessed by Kaiser test.[81] *N*-Fmoc deprotection was performed by treatment piperidine/DMF (1 : 4 v/v, 10 mL g^{-1} resin, 4 × 3 min). The cleavage was performed by treating the resin with TFA/MeOH (1 : 99 v/v, 10 × 2 min). The cleavage solutions were neutralised by addition to pyridine/MeOH (1 : 9 v/v, 20 mL), concentrated to small volume and precipitated from ice-cold water. The precipitate was washed again with ice cold water (20 mL) and dried *in vacuo*. The residue was dissolved in the minimum of methylene chloride and precipitated from diethyl ether. The white solid was triturated diethyl ether to obtain the crude peptide that was used in the next step without further purification. The cleavage performed onto 500 mg of peptidyl resin afforded 150 mg of crude peptide (40% based on loading of first residue). RP-HPLC (detector: λ = 220 nm): t_R = 9.87 min; ESI-MS (*m/z*): calcd. for $C_{45}H_{68}N_{11}O_{11}S$: 970.4815; found: 970.4712 [M + H]$^+$.

Peptide H-D(tBu)fK(Boc)R(Pmc)G-OH

Cleavage performed onto 500 mg of peptidyl resin afforded 220 mg (0.19 mmol) of crude peptide as a white solid (54% based on loading of the first residue). RP-HPLC (detector: λ = 220 nm): t_R = 10.07 min; ESI-MS (*m/z*): calcd. for $C_{50}H_{78}N_9O_{13}S$: 1044.5362, found: 1044.5086 [M + H]$^+$.

General procedure for cyclization reactions. Peptide cyclo[D(tBu)fK(ε-N$_3$)R(Pmc)G]

A 0.5 mM solution of linear protected peptide **18**, whose pH value was adjusted to 8–9 by addition of DIPEA, was treated with PyBOP (1 equiv). The solution was stirred at room temperature for 1 h. Solvent was removed under reduced pressure and the residue dissolved in the minimum of methylene chloride. Diethyl ether was added to precipitate crude peptide, which was triturated and washed with diethyl ether (3 × 10 mL), and in the next step without further purification. RP-HPLC (λ = 220 nm): t_R = 11.57 min; ESI-MS (*m/z*): calcd. for $C_{45}H_{65}N_{11}O_{10}S$: 951.4637; found: 951.4592 [M + H]$^+$.

Peptide cyclo[D(tBu)fK(Boc)R(Pmc)G]

White solid, RP-HPLC (detector: λ = 220 nm): t_R = 11.47 min; ESI-MS (*m/z*): calcd. for $C_{50}H_{75}N_9O_{12}S$: 1025.5256; found: 1025.5140 [M + H]$^+$.

General procedure for the deprotection of the peptides. Peptide cyclo[DfK(ε-N$_3$)RG]

Protected peptide **18** (72 mg) was treated with TFA/TIS/water (95/2.5/2.5, 1 mL) at room temperature for 2 h. The solvent were evaporated in reduced pressure and the residue was taken in a TFA (0.2 mL) and precipitated with diethyl ether (10 mL). Washing with diethyl ether was repeated 3 times, and the crude peptide was purified by Supelco Discovery DSC-18 cartridges (1 g), eluting with 0.1% TFA in acetonitrile/water (5/95). The solvent was evaporated and the residue was taken in MeOH. The solid residue was filtered off, and the TFA salt of the peptide was precipitated from the solution by addition of diethyl ether, yielding a white solid (58 mg, 82%) RP-HPLC (detector: λ = 220 nm): t_R = 6.33 min; ESI-MS: ($C_{27}H_{41}N_9O_7$ requires 603.3129).

Peptide cyclo[DfKRG]

The deprotection was performed onto 80 mg of protected cyclopeptide. White solid (68 mg, 86%). RP-HPLC (detector: λ = 220 nm): t_R = 5.80 min; ESI-MS (*m*/*z*): calcd. for $C_{27}H_{41}N_9O_7$: 603.3129; found: 603.3093 $[M + H]^+$.

Synthesis of cyclopeptide 19

To a solution of **cyclo[DfKRG]** (30 mg) in 20 mL of DMF/DCM (1/1 v/v), 1,1′-thiocarbonyldi-2(1H)piridone (8 mg, 0.04 mmol) was added, and the solution was stirred at room temperature for 3 h. DCM was evaporated *in vacuo*, and the resulting solution was added to diethyl ether (50 mL). The precipitate was collected by centrifugation and triturated with diethyl ether, to afford the desired peptide which was used for the conjugation reactions without further purification. White solid (25 mg, 77%). RP-HPLC (detector: λ = 220 nm): t_R = 7.38 min; ESI-MS (*m*/*z*): calcd. for $C_{28}H_{39}N_9O_7S$: 645.2693; found: 645.2720 $[M + H]^+$.

General procedure for the synthesis of functionalised polyacrylamide nanoparticles: alkyne-functionalised nanoparticles 6

Degassed hexane (42 mL) was added to a stirred solution of Brij® 30 (3.08 g, 8.5 mmol) and dioctyl sulfosuccinate sodium salt (1.59 g, 3.6 mmol). The mixture was allowed to stir under argon until complete dissolution of the surfactants. A solution of acrylamide (527 mg, 7.6 mmol), **4** (13 mg, 0.08 mmol), and N,N′-methylenebisacrylamide (160 mg, 1.0 mmol) in water (1.8 mL) was added to the hexane mixture. 10% aqueous ice-cold ammonium persulfate (30 μL) was added to the reaction vessel, followed by N,N,N′,N′-tetramethylethylenediamine (15 μL), and the reaction mixture allowed to stir at room temperature under argon for two hours. Excess hexane was evaporated *in vacuo*, and the resulting white viscous liquid was washed with ethanol and centrifuged (7 × 50 ml, 10 min, 4000 rpm). The solid was taken in ethanol and isolated by filtration through membrane, and dried *in vacuo* to yield the desired alkyne functionalized nanospecies as a white solid (621 mg, 88%). PCS z_{ave} (nm): nm 40.0 (deionised water).

Azide-functionalised nanoparticles 5

White solid (567 mg, 81%). PCS z_{ave} (nm): 37.6 (deionised water).

General procedure for the synthesis of doubly-functionalised polyacrylamide nanoparticles: alkyne-amine bifunctionalized nanoparticles 15

The synthesis of PANPs displaying two reactive functionalities was performed according to the general procedure reported above, adding commercially available 3-aminopropylacrylamide to the aqueous solution of acrylamide monomers, according to the following proportions: acrylamide (527 mg), N,N′-methylenebisacrylamide (160 mg), 3-aminopropylacrylamide (7 mg), acrylamide **4** (6 mg). The desired doubly-functionalised nanospecies were obtained as a white solid (609 mg, 87%). PCS z_{ave} (nm) 39.8.

Azide-amine bifunctionalized nanoparticles 14

White solid (647 mg, 92%). PCS z_{ave} (nm) 43.8.

Alkyne-amine bifunctionalized nanoparticles embedding aminodextran-conjugated CG-1 30

The synthesis of PANPs displaying two reactive functionalities was performed according to the general procedure reported above, replacing 40 μL of water in the aqueous solution with 40 μL of a 5 mg mL^{-1} aqueous solution of aminodextran-conjugated calcium green 1. The desired particles were obtained as a pale pink solid. (647 mg, 92%). PCS z_{ave} (nm) 37.7.

General procedure for the conjugation of amino-reactive porphyrins and peptides to bifunctionalised nanoparticles: nanoconjugates 21

Amino/alkyne-functionalised nanospecies **15** (100 mg) and were dispersed in deionised water (20 mL). To the solution, porphyrin **16** (2 mg, 2.1 × 10^{-3} mmol) was added, followed by TEA (20 μL, 1.4 × 10^{-4} mmol). The resulting mixture was shielded from light and shaken for 2 h on a rotating shaker. The desired conjugated species were purified by gel filtration. Ethanol was added to the eluate, and the particles were isolated by filtration through membrane and dried *in vacuo*. (Green solid, 82 mg, 82% recovery). PCS z_{ave} (nm) 99.8; UV/vis: (H_2O) λ (%): 442 (100), 567 (19.3), 613 (15.0).

Nanospecies 23

The conjugated nanospecies were obtained following the general procedure, using nanospecies **15** (100 mg) and peptide **19** (4 mg, 6.3 × 10^{-3} mmol). The desired nanoparticles were obtained as a white solid. (70 mg, 70% recovery. PCS z_{ave} (nm) 89.5.

Nanoconjugates 25

The conjugated nanospecies were obtained following the general procedure, using nanoparticles **14** (100 mg) and peptide **19** (4 mg, 6.3 × 10^{-3} mmol). The desired nanoparticles were obtained as a white solid. (74 mg, 74% recovery, PCS z_{ave} (nm) 103.1.

Nanoconjugates 27

The conjugated nanospecies were obtained following the general procedure, using nanoparticles **15** (100 mg) and porphyrin **16** (2 mg, 2.1 × 10^{-3} mmol). The desired nanoparticles were obtained as a green solid. (79 mg, 79% recovery, PCS z_{ave} (nm) 110.1).

General procedure for the CuAAC reaction-based conjugation of porphyrins to azide or alkyne-functionalised PANPs: nanoconjugates 12

Nanoparticles **5** (60 mg) and were dispersed in deionised water (9 mL). To the solution, porphyrin **7** (2 mg, 2.1 × 10^{-3} mmol) was added, followed by 10 mM aqueous $CuSO_4$ (250 μL, 2.5 mmol) and 100 mM aqueous sodium ascorbate (250 μL, 25 mmol). The resulting mixture was shielded from light and shaken overnight on a rotating shaker. The desired conjugated species were

purified by gel filtration. Ethanol was added to the eluate, and the particles were isolated by filtration through membrane and dried *in vacuo*. Green solid, 57 mg, 95% recovery, PCS z_{ave} (nm) 102.3; UV/vis: (H_2O) λ (%): 442 (100), 566 (20.3), 611 (15.7).

Nanoconjugates 13

Green solid, 50 mg, 83% recovery. PCS z_{ave} (nm) 92.3; UV/vis: (H_2O) λ (%): 443 (100), 567 (17.1), 613 (13.0).

Nanoconjugates 22

Nanoconjugates **21** (60 mg) and were dispersed in deionised water (9 mL). To the solution, peptide **18** (4 mg, 6.3×10^{-3} mmol) was added, followed by 10 mM aqueous $CuSO_4$ (250 μL, 2.5 mmol) and 100 mM aqueous sodium ascorbate (250 μL, 25 mmol). The resulting mixture was shielded from light and shaken overnight on a rotating shaker. The desired conjugated species were purified by gel filtration. Ethanol was added to the eluate, and the particles were isolated by filtration through membrane and dried *in vacuo*. (Green solid, 55 mg, 92% recovery). PCS z_{ave} (nm) 96.9; UV/vis: (H_2O) λ (%): 442 (100), 566 (18.6), 618 (16.4).

Nanoconjugates 24

The conjugated nanospecies were obtained following the general procedure, using nanoconjugates **23** (70 mg) and porphyrin **8** (4 mg, 4.1×10^{-3} mmol). The desired nanoconjugates were obtained as a green solid (63 mg, 90% recovery). PCS z_{ave} (nm) 70.0; UV/vis: (H_2O) λ (%): 442 (100), 567 (13.5), 612 (10.9).

Nanoconjugates 26

The conjugated nanospecies were obtained following the general procedure, using nanospecies **25** (80 mg) and porphyrin **7** (4 mg, 4.1×10^{-3} mmol). The desired nanoparticles were obtained as a green solid (67 mg, 97% recovery). PCS z_{ave} (nm) 92.7; UV/vis: (H_2O) λ (%): 442 (100), 566 (17.8), 613 (11.4).

Nanoconjugates 28

The conjugated nanospecies were obtained following the general procedure, using nanospecies **21** (60 mg) and 1-α-propargyloxy-mannose **20** (4 mg, 1.8×10^{-2} mmol). The desired nanoparticles were obtained as a green solid (54 mg, 90% recovery). PCS z_{ave} (nm) 98.4; UV/vis: (H_2O) λ (%): 443 (100), 567 (16.3), 613 (16.4).

Nanoconjugates 29

The conjugated nanospecies were obtained following the general procedure, using nanospecies **23** (60 mg) and **17** (3 mg, 2.7×10^{-2} mmol). The solvent for this reaction was 10% aqueous DMSO. The desired nanoparticles were obtained as a blue solid (54 mg, 91% recovery). PCS z_{ave} (nm) 69.2; UV/vis: (H_2O) λ (%): 651 (94.6), 701 (100).

Synthesis of nanoconjugates 31

Nanospecies **30** (100 mg) and were dispersed in deionised water (15 mL). To the solution, porphyrin **16** (1 mg, 1.0×10^{-3} mmol) was added, followed by TEA (50 μL, 3.6×10^{-4} mmol). The resulting mixture was shielded from light and shaken for 2 h on a rotating shaker. The solution was filtered through Sephadex, and to the green eluate containing the porphyrin-coated nanoparticles, an aqueous solution of peptide **18** (10 mg mL^{-1}, 500 μL, 7.9×10^{-3} mmol) was added, followed by 10 mM aqueous $CuSO_4$ (250 μL, 2.5 mmol) and 100 mM aqueous sodium ascorbate (250 μL, 25 mmol). The resulting mixture was shielded from light and it was shaken overnight on a rotating shaker. The desired conjugated species were isolated by gel filtration and precipitation with ethanol. Filtration through membrane and drying *in vacuo* yielded the desired nanoparticles. (Green solid, 88 mg, 88% recovery). PCS z_{ave} (nm) 71.7; UV/vis: (H_2O) λ (%): 439 (100), 567 (18.3), 618 (22.5).

Sakaguchi test

The assay is based on the method described by Michael *et al.*,[79] with minor modifications. Solutions: Reagent A: 5% urea and 0.05% 1-naphthol in 95% ethanol. Reagent B: 0.7% bromine in 1.25 M NaOH. 5 mg mL^{-1} solutions of RGD-coated nanospecies in deionised water were used as the samples. Positive control samples were prepared using 1 mM Arg in deionised water. Deionised water and 5 mg mL^{-1} suspension of nanospecies **15** in deionised water were used as negative controls. Method: 250 μL of sample solution were added to 250 μL of reagent A, followed by 500 μL of reagent B in an eppendorf tube. The mixture was mixed on a vortex shaker and then it was allowed to stand at room temperature for 5 min. The solution was then transferred in a quartz cuvette (1 mL) and the absorption spectrum was recorded between 250 and 750 nm. The test was considered positive when $I_{sample}/I_{Q-1} > 2$ at 480 nm.

Phenol-sulfuric acid test

The assay was based on the micro-method described by Masuko *et al.*[77] Solutions: Reagent A: 5% phenol in deionised water. Reagent B: concentrated H_2SO_4 (1.14 g mL^{-1}). 5 mg mL^{-1} solutions of nanospecies **27** in deionised water was used as analyte solution. Positive control samples were prepared using 10 mM mannose in deionised water. Deionised water (control C) and 5 mg mL^{-1} suspension of nanospecies **15** in deionised water (control D) were used as negative controls. Method: 450 μL of reagent B were added to 150 μL of the analyte solution, followed by 90 μL of reagent A in a test tube equipped with a stopper. The mixture was mixed on a vortex shaker and then it was transferred into a graphite bath and allowed to stand at 90 °C for 10 min. The solution was then transferred in a quartz cuvette (1 mL) and the absorbance of the sample was recorded between 400 and 550. The test was considered positive when $I_{sample}/I_{Q-1} > 2$ at 450 nm.

Abbreviations

APMA	*N*-(3-aminopropyl)methacrylamide hydrochloride
CG-1	calcium green 1
CuAAC	copper-catalysed alkyne-azide cycloaddition
DCM	dichloromethane
DIPEA	diisopropylethylamine
DMF	*N*,*N*-dimethylformamide

DMSO	dimethylsulfoxide
PANPs	polyacrylamide nanoparticles
PCS	photon correlation spectroscopy
PyBOP	benzotriazol-1-yl-oxytripyrrolidinophosphonium hexafluorophosphate
SPE	solid phase extraction
SPPS	solid phase peptide synthesis
TAMRA	carboxytetramethylrhodamine
TBAC	tetrabutylammonium chloride
TBTA	tris-(benzyltriazolylmethyl)amine
TEA	triethylamine
TFA	trifluoroacetic acid
THF	tetrahydrofuran
TIS	triisopropylsilane
TLC	thin layer chromatography

Acknowledgements

The authors thank EPSRC for funding the project (EP/H000151/1) and EPSRC Mass Spectrometry Service, Swansea for analyses. F.G. thanks Mr Mark Ward for the helpful discussions about microemulsion polymerisation.

References

1 D. Gao, H. Xu, M. A. Philbert and R. Kopelman, *Angew. Chem., Int. Ed.*, 2007, **46**, 2224–2227.
2 D. Gao, H. Xu, M. A. Philbert and R. Kopelman, *Nano Lett.*, 2008, **8**, 3320–3324.
3 M. Hamidi, A. Azadi and P. Rafiei, *Adv. Drug Delivery Rev.*, 2008, **60**, 1638–1649.
4 M. Kuruppuarachchi, H. Savoie, A. Lowry, C. Alonso and R. W. Boyle, *Mol. Pharmaceutics*, 2011, **8**, 920–931.
5 M. Qin, H. J. Hah, G. Kim, G. Nie, Y.-E. K. Lee and R. Kopelman, *Photochem. Photobiol. Sci.*, 2011, **10**, 832–841.
6 R. L. Juliano, X. Ming, O. Nakagawa, R. Xu and H. Yoo, *Theranostics*, 2011, **1**, 211–219.
7 H. Sun, A. M. Scharff-Poulsen, H. Gu, I. Jakobsen, J. M. Kossmann, W. B. Frommer and K. Almdal, *ACS Nano*, 2008, **2**, 19–24.
8 G. R. Reddy, M. S. Bhojani, P. McConville, J. Moody, B. A. Moffat, D. E. Hall, G. Kim, Y.-E. L. Koo, M. J. Woolliscroft, J. V. Sugai, T. D. Johnson, M. A. Philbert, R. Kopelman, A. Rehemtulla and B. D. Ross, *Clin. Cancer Res.*, 2006, **12**, 6677–6686.
9 J. K. Oh, R. Drumright, D. J. Siegwart and K. Matyjaszewski, *Prog. Polym. Sci.*, 2008, **33**, 448–477.
10 N. Munshi, T. K. De and A. Maitra, *J. Colloid Interface Sci.*, 1997, **190**, 387–391.
11 A. Vakurov, N. A. Pchelintsev, J. Forde, C. Ó'Fágáin, T. Gibson and P. Millner, *Nanotechnology*, 2009, **20**, 295605.
12 O. B. Locos, C. C. Heindl, A. Corral, M. O. Senge and E. M. Scanlan, *European J. Org. Chem.*, 2010, **2010**, 1026–1028.
13 R. Minchin, *Nat. Nanotechnol.*, 2008, **3**, 12–13.
14 S.-Y. Lin, C.-h. Chen, M.-C. Lin and H.-F. Hsu, *Anal. Chem.*, 2005, **77**, 4821–4828.
15 S. C. Abeylath, S. Ganta, A. K. Iyer and M. Amiji, *Acc. Chem. Res.*, 2011, **44**, 1009–1017.
16 H. Koo, M. S. Huh, I.-C. Sun, S. H. Yuk, K. Choi, K. Kim and I. C. Kwon, *Acc. Chem. Res.*, 2011, **44**, 1018–1028.
17 K. Welser, J. Grilj, E. Vauthey, J. W. Aylott and W. C. Chan, *Chem. Commun.*, 2009, 671–673.
18 W. R. Algar, D. E. Prasuhn, M. H. Stewart, T. L. Jennings, J. B. Blanco-Canosa, P. E. Dawson and I. L. Medintz, *Bioconjugate Chem.*, 2011, **22**, 825–858.
19 M. Breunig, S. Bauer and A. Goepferich, *Eur. J. Pharm. Biopharm.*, 2008, **68**, 112–128.
20 D. Bechet, P. Couleaud, C. Frochot, M.-L. Viriot, F. Guillemin and M. Barberi-Heyob, *Trends Biotechnol.*, 2008, **26**, 612–621.
21 E. Paszko, C. Ehrhardt, M. O. Senge, D. P. Kelleher and J. V. Reynolds, *Photodiagn. Photodyn. Ther.*, 2011, **8**, 14–29.
22 Y. Cheng and C. Burda, in *Comprehensive Nanoscience and Technology*, ed. D. Andrews, G. Scholes and G. Wiederrecht, Academic Press, Amsterdam, 2011, pp. 1–28.
23 D. K. Chatterjee, L. S. Fong and Y. Zhang, *Adv. Drug Delivery Rev.*, 2008, **60**, 1627–1637.
24 C. I. Olariu, H. H. P. Yiu, L. Bouffier, T. Nedjadi, E. Costello, S. R. Williams, C. M. Halloran and M. J. Rosseinsky, *J. Mater. Chem.*, 2011, **21**, 12650–12659.
25 Y. H. Lau, P. J. Rutledge, M. Watkinson and M. H. Todd, *Chem. Soc. Rev.*, 2011, **40**, 2848–2866.
26 J. W. Aylott, *Analyst*, 2003, **128**, 309–312.
27 H. A. Clark, M. Hoyer, M. A. Philbert and R. Kopelman, *Anal. Chem.*, 1999, **71**, 4831–4836.
28 H. A. Clark, R. Kopelman, R. Tjalkens and M. A. Philbert, *Anal. Chem.*, 1999, **71**, 4837–4843.
29 H. Xu, S. M. Buck, R. Kopelman, M. A. Philbert, M. Brasuel, B. D. Ross and A. Rehemtulla, *Isr. J. Chem.*, 2004, **44**, 317–337.
30 M. Brasuel, R. Kopelman, J. W. Aylott, H. Clark, H. Xu, M. Hoyer, T. J. Miller, R. Tjalkens and M. A. Philbert, *Sensor. Mater.*, 2002, **14**, 309–338.
31 L. B. Josefsen, J. W. Aylott, A. Beeby, P. Warburton, J. P. Boyle, C. Peers and R. W. Boyle, *Photochem. Photobiol. Sci.*, 2010, **9**, 801–811.
32 P. J. Cywinski, A. J. Moro, S. E. Stanca, C. Biskup and G. J. Mohr, *Sens. Actuators, B*, 2009, **135**, 472–477.
33 A. Fercher, S. M. Borisov, A. V. Zhdanov, I. Klimant and D. B. Papkovsky, *ACS Nano*, 2011, **5**, 5499–5508.
34 Y.-E. Koo Lee, E. E. Ulbrich, G. Kim, H. Hah, C. Strollo, W. Fan, R. Gurjar, S. Koo and R. Kopelman, *Anal. Chem.*, 2010, **82**, 8446–8455.
35 Y.-E. L. Koo, Y. Cao, R. Kopelman, S. M. Koo, M. Brasuel and M. A. Philbert, *Anal. Chem.*, 2004, **76**, 2498–2505.
36 X.-d. Wang, H. H. Gorris, J. A. Stolwijk, R. J. Meier, D. B. M. Groegel, J. Wegener and O. S. Wolfbeis, *Chem. Sci.*, 2011, **2**, 901–906.
37 H. Zhang, Y. Sun, K. Ye, P. Zhang and Y. Wang, *J. Mater. Chem.*, 2005, **15**, 3181–3186.
38 X. Zhou, F. Su, Y. Tian, R. H. Johnson and D. R. Meldrum, *Sens. Actuators, B*, 2011, **159**, 135–141.
39 Q. Yan, J. Yuan, Y. Kang, Z. Cai, L. Zhou and Y. Yin, *Chem. Commun.*, 2010, **46**, 2781–2783.
40 W. Tan, Z.-Y. Shi and R. Kopelman, *Sens. Actuators, B*, 1995, **28**, 157–163.
41 R. K. O'Reilly, C. J. Hawker and K. L. Wooley, *Chem. Soc. Rev.*, 2006, **35**, 1068–1083.
42 L. Levy, Y. Sahoo, K.-S. Kim, E. J. Bergey and P. N. Prasad, *Chem. Mater.*, 2002, **14**, 3715–3721.
43 M. J. Moreno, E. Monson, R. G. Reddy, A. Rehemtulla, B. D. Ross, M. Philbert, R. J. Schneider and R. Kopelman, *Sens. Actuators, B*, 2003, **90**, 82–89.
44 V. Alexander, A. P. Nikolay, F. Jessica, Ó. F. Ciaran, G. Tim and M. Paul, *Nanotechnology*, 2009, **20**, 295605.
45 A. R. de Luzuriaga, N. Ormategui, H. J. Grande, I. Odriozola, J. A. Pomposo and I. Loinaz, *Macromol. Rapid Commun.*, 2008, **29**, 1156–1160.
46 J. Lu, M. Shi and M. S. Shoichet, *Bioconjugate Chem.*, 2008, **20**, 87–94.
47 S. Deshayes, V. Maurizot, M.-C. Clochard, C. Baudin, T. Berthelot, S. Esnouf, D. Lairez, M. Moenner and G. Déléris, *Pharm. Res.*, 2011, **28**, 1631–1642.
48 K. Welser, M. D. A. Perera, J. W. Aylott and W. C. Chan, *Chem. Commun.*, 2009, 6601–6603.
49 S. Binauld, D. Damiron, L. A. Connal, C. J. Hawker and E. Drockenmuller, *Macromol. Rapid Commun.*, 2011, **32**, 147–168.
50 R. K. Iha, K. L. Wooley, A. M. Nyström, D. J. Burke, M. J. Kade and C. J. Hawker, *Chem. Rev.*, 2009, **109**, 5620–5686.
51 M. Malkoch, R. J. Thibault, E. Drockenmuller, M. Messerschmidt, B. Voit, T. P. Russell and C. J. Hawker, *J. Am. Chem. Soc.*, 2005, **127**, 14942–14949.
52 K. Nilles and P. Theato, *J. Polym. Sci., Part A: Polym. Chem.*, 2010, **48**, 3683–3692.

53 R. K. O'Reilly, M. J. Joralemon, C. J. Hawker and K. L. Wooley, *New J. Chem.*, 2007, **31**, 718–724.
54 I. Singh, Z. Zarafshani, F. Heaney and J.-F. Lutz, *Polym. Chem.*, 2011, **2**, 372–375.
55 J. M. Spruell, M. Wolffs, F. A. Leibfarth, B. C. Stahl, J. Heo, L. A. Connal, J. Hu and C. J. Hawker, *J. Am. Chem. Soc.*, 2011, **133**, 16698–16706.
56 M. A. Azagarsamy, V. Yesilyurt and S. Thayumanavan, *J. Am. Chem. Soc.*, 2010, **132**, 4550–4551.
57 V. V. Rostovtsev, L. G. Green, V. V. Fokin and K. B. Sharpless, *Angew. Chem.*, 2002, **114**, 2708–2711.
58 P. Beck, D. Scherer and J. Kreuter, *J. Microencapsulation*, 1990, **7**, 491–496.
59 S. Udenfriend, S. Stein, P. Böhlen, W. Dairman, W. Leimgruber and M. Weigele, *Science*, 1972, **178**, 871–872.
60 J. M. Sutton, O. J. Clarke, N. Fernandez and R. W. Boyle, *Bioconjugate Chem.*, 2002, **13**, 249–263.
61 X. Montet, M. Funovics, K. Montet-Abou, R. Weissleder and L. Josephson, *J. Med. Chem.*, 2006, **49**, 6087–6093.
62 W. Chen, P. A. Jarzyna, G. A. F. van Tilborg, V. A. Nguyen, D. P. Cormode, A. Klink, A. W. Griffioen, G. J. Randolph, E. A. Fisher, W. J. M. Mulder and Z. A. Fayad, *FASEB J.*, 2010, **24**, 1689–1699.
63 F. Danhier, B. Vroman, N. Lecouturier, N. Crokart, V. Pourcelle, H. Freichels, C. Jérôme, J. Marchand-Brynaert, O. Feron and V. Préat, *J. Controlled Release*, 2009, **140**, 166–173.
64 E. A. Murphy, B. K. Majeti, L. A. Barnes, M. Makale, S. M. Weis, K. Lutu-Fuga, W. Wrasidlo and D. A. Cheresh, *Proc. Natl. Acad. Sci. U. S. A.*, 2008, **105**, 9343–9348.
65 R. Kopelman, Y.-E. Lee Koo, M. Philbert, B. A. Moffat, G. Ramachandra Reddy, P. McConville, D. E. Hall, T. L. Chenevert, M. S. Bhojani, S. M. Buck, A. Rehemtulla and B. D. Ross, *J. Magn. Magn. Mater.*, 2005, **293**, 404–410.
66 R. Su, L. Li, X. Chen, J. Han and S. Han, *Org. Biomol. Chem.*, 2009, **7**, 2040–2045.
67 J. Rieger, H. Freichels, A. Imberty, J. L. Putaux, T. Delair, C. Jeérôme and R. Auzeély-Velty, *Biomacromolecules*, 2009, **10**, 651–657.
68 D. Brevet, M. Gary-Bobo, L. Raehm, S. Richeter, O. Hocine, K. Amro, B. Loock, P. Couleaud, C. Frochot, A. Morere, P. Maillard, M. Garcia and J.-O. Durand, *Chem. Commun.*, 2009, 1475–1477.
69 C.-C. Lin, Y.-C. Yeh, C.-Y. Yang, C.-L. Chen, G.-F. Chen, C.-C. Chen and Y.-C. Wu, *J. Am. Chem. Soc.*, 2002, **124**, 3508–3509.
70 D. Boturyn and P. Dumy, *Tetrahedron Lett.*, 2001, **42**, 2787–2790.
71 C. Byrne, P. A. McEwan, J. Emsley, P. M. Fischer and W. C. Chan, *Chem. Commun.*, 2011, **47**, 2589–2591.
72 S. Kim and K. Y. Yi, *J. Org. Chem.*, 1986, **51**, 2613–2615.
73 See Supplementary Information† for experimental details.
74 M. R. Gittings and D. A. Saville, *Colloids Surf., A*, 1998, **141**, 111–117.
75 G. A. Schumacher and T. G. M. van de Ven, *Faraday Discuss. Chem. Soc.*, 1987, **83**, 75–85.
76 K. McAllister, P. Sazani, M. Adam, M. J. Cho, M. Rubinstein, R. J. Samulski and J. M. DeSimone, *J. Am. Chem. Soc.*, 2002, **124**, 15198–15207.
77 T. Masuko, A. Minami, N. Iwasaki, T. Majima, S.-I. Nishimura and Y. C. Lee, *Anal. Biochem.*, 2005, **339**, 69–72.
78 J. D. Mold, J. M. Ladino and E. J. Schantz, *J. Am. Chem. Soc.*, 1954, **75**, 6321–6322.
79 J. Michael, L. Schönzart, I. Israel, R. Beutner, D. Scharnweber, H. Worch, U. Hempel and B. Schwenzer, *Bioconjugate Chem.*, 2009, **20**, 710–718.
80 D. B. G. Williams and M. Lawton, *J. Org. Chem.*, 2010, **75**, 8351–8354.
81 E. Kaiser, R. L. Colescott, C. D. Bossinger and P. I. Cook, *Anal. Biochem.*, 1970, **34**, 595–598.